Separation Science and Technology
Publication details, including instructions for authors and subscription information:
http://www.informaworld.com/smpp/title~content=t713708471

Adsorption of Carbon Dioxide onto EDA-CP-MS41

Kyu-Suk Hwang[a]; Young-Sik Son[a]; Sang-Wook Park[a]; Dae-Won Park[a]; Kwang-Joong Oh[a]; Seong-Soo Kim[b]
[a] Division of Chemical Engineering, Pusan National University, Busan, Korea [b] School of Environmental Science, Catholic University of Pusan, Busan, Korea

Online publication date: 07 January 2010

To cite this Article Hwang, Kyu-Suk , Son, Young-Sik , Park, Sang-Wook , Park, Dae-Won , Oh, Kwang-Joong and Kim, Seong-Soo(2010) 'Adsorption of Carbon Dioxide onto EDA-CP-MS41', Separation Science and Technology, 45: 1, 85 — 93
To link to this Article: DOI: 10.1080/01496390903401804
URL: http://dx.doi.org/10.1080/01496390903401804

Separation Science and Technology, 45: 85–93, 2010

ISSN: 0149-6395 print/1520-5754 online
DOI: 10.1080/01496390903401804

Taylor & Francis
Taylor & Francis Group

Adsorption of Carbon Dioxide onto EDA-CP-MS41

Kyu-Suk Hwang,[1] Young-Sik Son,[1] Sang-Wook Park,[1] Dae-Won Park,[1] Kwang-Joong Oh,[1] and Seong-Soo Kim[2]

[1]*Division of Chemical Engineering, Pusan National University, Busan, Korea*
[2]*School of Environmental Science, Catholic University of Pusan, Busan, Korea*

Carbon dioxide was adsorbed onto mesoporous adsorbent of ethylene diamine immobilized CP-MCM41 (EDA-CP-MS41), which was synthesized by chloropropyl functionalized MCM-41 (CP-MS41) with ethylene diamine, in a laboratory-scale packed-bed. The adsorber was operated batchwise with the charge of adsorbent in the range of 1–3 g to obtain the breakthrough curves of CO_2. Experiments were carried out at different adsorption temperatures (30–50°C) and flow rates of nitrogen (15–60 cm^3/min) to investigate the effects of these experimental variables on the breakthrough curves. The deactivation model was tested for these curves by combining the adsorption of CO_2 and the deactivation of adsorbent particles. The observed values of the adsorption rate constant and the deactivation rate constant were evaluated through analysis of the experimental breakthrough data using a nonlinear least squares technique. The experimental breakthrough data were fitted very well to the deactivation model than the adsorption isotherm models in the literature.

Keywords breakthrough curve; carbon dioxide; deactivation model; mesoporous adsorbent

INTRODUCTION

Carbon dioxide (CO_2) produced by combustion of fossil fuels is regarded as the most significant greenhouse gas with its increasing accumulation in the atmosphere attracting worldwide attention (1). Various methods have been used to remove it: absorption by solvent and adsorption by molecular sieve, membrane separation, and cryogenic fractionation. In particular, absorption has been widely used in the chemical industries, as with the Benfield Process (2). Adsorption is one of the most widely employed methods in practical industrial operation because of the easy operation and low cost with efficient recovery of the solute (3). The most important characteristics of porous adsorbents are their surface properties such as porous structure, pore size distribution, wall thickness, specific surface area, and hydrophilic-hydrophobic properties. The discovery of the M41S family by a Mobil scientist (4, 5) generated a great deal of interest in the synthesis of organically-functionalized, mesoporous materials for their application in the fields of catalysis, sensing, and adsorption, given their high surface areas and large ordered pores ranging from 20 to 100 Å (5) with narrow size distributions. High chemical and thermal stabilities also make them potential and promising candidates for the reactions of bulky substrate molecules. In general, hybrid organic-inorganic materials have been prepared via post-grafting or co-condensation techniques. In 2000, Bhaumik and Tatsumi (6) reported a grafting technique through a co-condensation method for hybrid MCM-41 using halogenated organosilanes. Recently, a new synthetic approach for the preparation of hybrid inorganic-organic mesoporous materials has been developed based on the co-condensation of siloxane and organosiloxane precursors in the presence of different templating surfactant solutions (4, 7–11). However, removing the surfactants by acid leaching leads to meso-structural disorder in the functionalized mesoporous materials (10). Although this methodology has been adopted for hybrid MCM-41, several studies (12–16) reported post-grafting techniques rather than a co-condensation method.

The idea of grafting functional groups onto the pore walls of silica and ordered mesoporous silica is a known strategy for the design of promising new adsorbents and catalysts. Although considerable research effort has been developed to the sweetening of sour natural gases, few studies have been reported on the performance of solid materials as sorbents for CO_2 and SO_2; chemisorption of sulfur dioxide (17) or carbon dioxide (18–24) amine-modified silica-gel.

The diffusion may have an effect on the reaction kinetics (25) in a non-catalytic heterogeneous gas-solid reaction such as adsorption that accompanies chemical reactions. It is complicated to analyze the experimental breakthrough data in a fixed bed, because reasonable diffusivity (26) of a solute and physical properties of solid particle need to be known. The conventional isotherm models (27, 28), such as the Langmuir, Freundlich, Brunauer-Emmett-Teller (BET), and Dubinin-Radushkevich-Kagener (DRK) model

Received 28 January 2009; accepted 31 August 2009.
Address correspondence to Sang-Wook Park, Division of Chemical Engineering, Pusan National University, Busan 609-735, Korea. Tel.: 82 51 510 2393; Fax: 82 51 512 8563. E-mail: swpark@pusan.ac.kr

have been used to obtain the adsorption kinetics, but it is difficult and tedious to prepare the experimental values of the sorption isotherm. Conversely, the deactivation model (DM) (29–31), as a simplified model, has been used to predict the breakthrough curve, assuming that the formation of a dense product layer over the surface of the adsorbent changed the number of active sites and the possible variations in the adsorption of active sites to cause a drop in the adsorption rate. This model makes the breakthrough curve analyzed easily and correlated with adsorption isotherm. Park et al. have investigated the reaction kinetics in carbonation of sodium carbonate (32) and potassium carbonate (33) with CO_2, and adsorption kinetics in adsorption of toluene vapor onto activated carbon (34) from analysis of the experimental breakthrough data in a fixed bed with DM.

To our knowledge, no literature report about analysis of adsorption kinetics onto amine-modified material from the experimental breakthrough data using DM to capture CO_2 has yet been published. Park et al. in the literatures, as mentioned above, have not used amine-modified material to capture CO_2. In this study, the solid particle of ethylene diamine-immobilized ionic liquid (EDA-CP-MS41) on the hybrid CP-MCM41, synthesized in the previous work (24), was used as an adsorbent of CO_2, which is one of the series of works (32–34) to investigate the adsorption kinetics from analysis of the experimental breakthrough data by DM and to present the relationship between the breakthrough data and the adsorption isotherm.

THEORY

The formation of a dense product layer over the solid adsorbent creates an additional diffusion resistance and is expected to cause a drop in the adsorption rate. One would also expect it to cause significant changes in the accessible pore volume, active surface area, and activity per unit area of solid adsorbent with respect to the extent of the adsorption. All of these changes cause a decrease of vacant surface area of the adsorbent with time. In DM, the effects of all of these factors on the diminishing rate of CO_2 capture are combined in a deactivation rate term.

With assumptions (34) of the pseudo-steady state and the isothermal species conservation equation for CO_2 in the fixed bed is

$$-Q_o \frac{dC_A}{dS} - k_o C_A \alpha = 0 \quad (1)$$

In writing this equation, axial dispersion in the fixed bed and any mass transfer resistances are assumed to be negligible. According to the proposed DM, the rate of change of the activity of the solid adsorbent is expressed as

$$-\frac{d\alpha}{dt} = k_d {C_A}^n \alpha^m \quad (2)$$

The zeroth solution of the deactivation models is obtained by taking $n = 0$. $m = 1$, and the initial activity of the solid as unity.

$$a = \exp[-k_o \tau \exp(-k_d t)] \quad (3)$$

Equation (3) is identical to the breakthrough equation proposed by Suyadal et al. (31) and assumes a fluid phase concentration that is independent of deactivation processes along the adsorber. More realistically, one would expect the deactivation rate to be concentration-dependent and, accordingly, axial-position-dependent in the fixed bed.

To obtain the analytical solution of Eq. (1) and (2) by taking $n = m = 1$, an iterative procedure is applied. The procedure used here is similar to the paper proposed by Dogu (35) for the approximate solution of nonlinear equations. In this paper, the zeroth solution of Eq. (3) is substituted into Eq. (2), and the first correction for the activity is obtained by the integration of this equation. Then, the corrected activity expression is substituted into Eq. (1), and integration of this equation gives the first corrected solution for the breakthrough curve.

$$a = \exp\left[\frac{[1 - \exp(k_o \tau(1 - \exp(-k_d t)))]}{1 - \exp(-k_d t)} \exp(-k_d t)\right] \quad (4)$$

This iterative procedure can be repeated for further improvement of the solution. In this procedure, higher-order terms in the series solutions of the integrals are neglected. The breakthrough curve for the deactivation model with two parameters ($k_o\tau$ and k_d) is calculated from the concentration profiles by Eq. (4).

EXPERIMENTAL

Chemicals

All chemicals were of reagent grade and were used without further purification. Purity of both CO_2 and N_2 was greater than 99.9%. Ethylene diamine (EDA), tetraethylorthosilicate (TEOS), 3-chloropropyltriethoxysilane (CITPES), cetyltrimethylammonium bromide (CTMABr), and tetramethylammounium hydroxide were supplied by Aldrich Chemical Company, U.S.A.

Synthesis of EDA-CP-MS41

CP-MS41 was synthesized by hydrolysis of TEOS, as a silicon source, with CITPES as an organosilane using CTMABr as a template. EDA-CP-MS41 was synthesized by immobilization of EDA on the mesoporous CP-MCM41. Both synthetic procedures of CP-MS41 and EDA-CP-MS41 followed previous work (16). FT-IR spectrum of CP-MS41 and EDA-CP-MS41 was shown in Fig. 1 to present characterization of the organic groups in the adsorbent. As shown in Fig. 1, EDA immobilized on CP-MS41 was observed from IR bands such as $-NH_2$ in

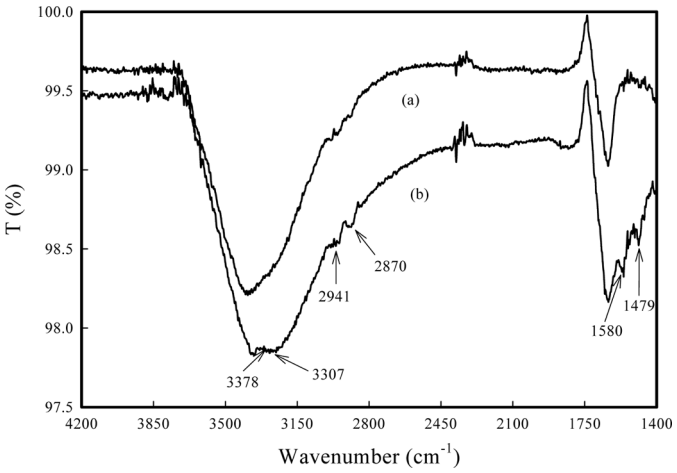

FIG. 1. FT-IR spectrum of CP-MCM41 (a) and EDA-CP-MS41.

the range of 3400–3300 cm^{-1} and 1600–1400 cm^{-1}, and -CH_2 in the range of 3000–2800 cm^{-1}. From the previous work, the measured values of the surface area by BET isotherm, particle size by SEM, pore diameter by N_2 adsorption using the BjH method, and micropore surface and micropore volume by t-plot method of CP-MS41 were 885 m^2/g, 5.0 μm, 28 Å, 105 m^2/g, and 0.06 cm^3/g, respectively. The adsorption-desorption isotherms of CP-MS41 was type IV in nature and indicated the presence of mesopores (20).

An Apparatus for CO_2 Capture and its Operation

An adsorption experiment (Fig. 2) was carried out in the presence of CO_2 with EDA-CP-MS41 adsorbent in a fixed bed pyrex glass reactor with internal diameter of 2 cm. CO_2 was carried by nitrogen gas through a sparger. The concentration of CO_2 in the nitrogen stream at the outlet of the sparger was measured by a gas chromatograph. The flow rate of gas mixture of CO_2 and nitrogen were within the range of 15–60 cm^3/min (measured at 25°C). The amount of adsorbent and the adsorption temperature were in the range of 1–3 g, 30–50°C, respectively. Experiments were repeated 3 times to obtain the average value for each type of experiment. A gas chromatograph (detector: thermal conductivity detector; column: Haysep D (10 feet by 1/8 inch of stainless steel; detector temperature: 190°C; feed temperature: 160°C; flow rate of He: 25.7 cm^3/min; retention time of N_2, CO_2: 1.497, 2.08 min, respectively.) connected to the exit stream of the adsorber allowed for on-line analysis of CO_2 and N_2.

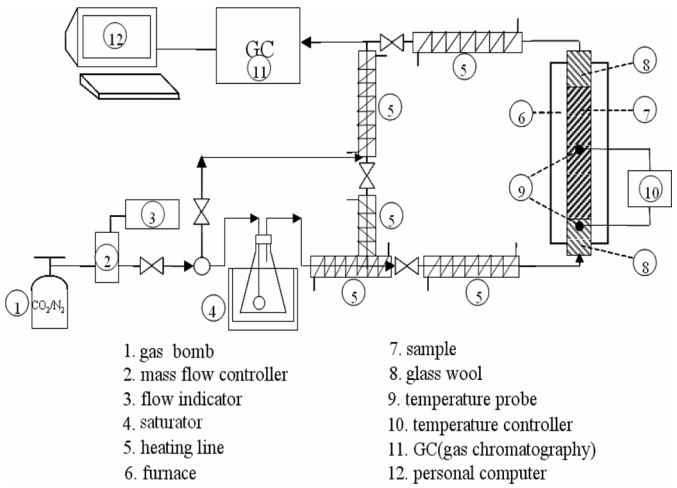

FIG. 2. Schematic diagram of a fixed bed apparatus.

EDA-CP-MS41 particles were supported by glass wool from both sides. The adsorber was placed into a tubular furnace equipped with a temperature controller. The length of the fixed adsorbent section of the bed was 5 cm of the adsorber. Temperature profiles were not observed within this section. All of the flow lines between the adsorber and the gas analyzer were heated to eliminate any condensation. Three-way valves placed before and after the adsorber allowed for flow of the gaseous mixture through the bypass line during flow rate adjustments. Composition of the inlet stream was checked by the analysis of the stream flowing through the bypass line at the start experiments. The experimental procedure used to obtain the breakthrough curve of CO_2 was the same as that reported in detail previously (34).

RESULTS AND DISCUSSION

To investigate the adsorption kinetics of CO_2 on EDA-CP-MS41 using two parameters of DM, the breakthrough curves of CO_2 were measured according to changes of the experimental variables such as flow rate of carrier gas, amount of adsorbent, and adsorption temperature.

Effect of Flow Rate of Gaseous Mixtures of CO_2 and N_2

To investigate the effect of flow rate of gaseous mixtures of CO_2 and N_2 on the kinetics, the breakthrough curves of CO_2 were measured in the range of flow rate of gaseous mixtures from 15–60 cm^3/min (measured at 25°C) under the typical experimental conditions such as 15% of CO_2 concentration, 30°C and 2 g of the adsorbent. The measured outlet concentrations of CO_2 were typically plotted against the adsorption time for the various flow rates indicated as various symbols in Fig. 3.

As shown in Fig. 3, a shift of breakthrough curves to shorter times was observed at a greater flow rate of the gaseous mixture with decrease in the amount of CO_2 that the bed can hold up to a certain breakthrough level. This result means that the adsorbed amount of CO_2 decreases as the space time of the gaseous mixtures in the fixed bed decreases. The breakthrough curve was evaluated by analysis of the experimental breakthrough data using a

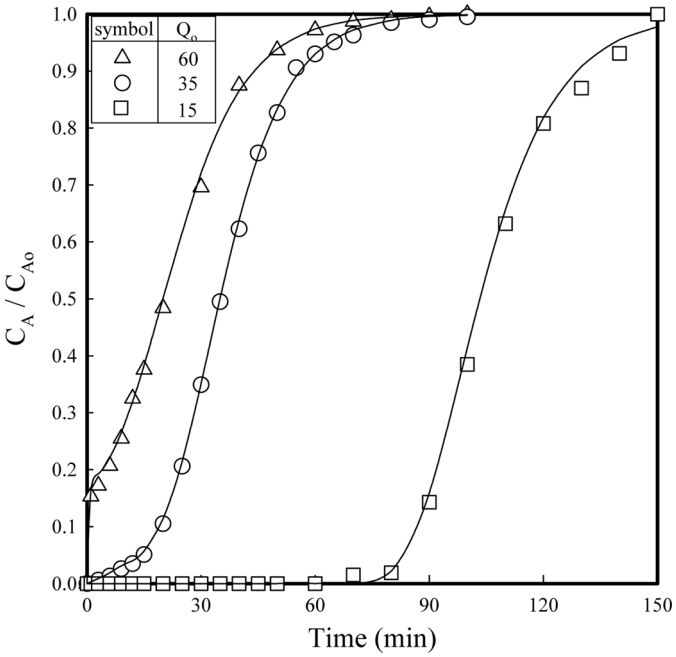

FIG. 3. Effect of flow rates of gaseous mixtures on the breakthrough curve of CO_2. ($y_A = 0.15$, $W = 2\,g$; $T = 30°C$).

nonlinear least squares technique with the parameters of k_d (tabulated in Table 1), and drawn as a solid line in Fig. 3. The standard deviations of the experimental $k_o\tau$ and k_d in Table 1 were added. As shown in Fig. 3, the regression analysis of the experimental breakthrough data gave very good agreement with the breakthrough equation Eq. (4) with regression coefficient more than 0.997. As shown in Table 1, the values of $k_o\tau$ decreased with increasing Q_o where the k_o's and k_d's were almost same.

Effect of Amount of EDA-CP-MS41

A set of experiments was performed to investigate the effect of the mass of EDA-CP-MS41 in the range from 1 to 3 g on the CO_2 breakthrough curves. As shown in Fig. 4, a good description of data was obtained by using Eq. (4) for each set of amount of EDA-CP-MS41 at y_A of 0.15, T of 30°C, and Q_o of 35 cm^3/min.

Also, the adsorbed amount of CO_2 increased with increasing the amount of EDA-CP-MS41. The model parameters determined from the analysis of the experimental breakthrough data are tabulated in Table 1. As shown in Table 1, the values of $k_o\tau$ increase with increasing W whereas the k_o's and k_d's are almost same.

Effect of Feedstock Concentration of CO_2

To determine the dependence of the adsorption parameters on the feedstock concentration of CO_2, the breakthrough curves of CO_2 were measured in the range of CO_2 concentration from 5–50% at flow rate of the gaseous mixture of 35 cm^3/min, temperature of 30°C, and EDA-CP-MS41 of 2 g. A good fitting of DM predictions to experimental data could be seen by inserting the corresponding values of the parameters tabulated in table 1 into Eq. (4) and was shown in Fig. 5. As shown in Fig. 5, the acceleration of the CO_2 breakthrough was observed with an increased feedstock concentration of CO_2. This behavior indicated a much quicker saturation of the adsorbent, because the EDA-CP-MS41 used in this study was relatively mesoporous, so that internal diffusion might have been a rate-limiting step in the kinetics of physical CO_2 adsorption.

TABLE 1
Rate parameters for various experimental conditions

T (°C)	Q_o (cm^3/min)	W (g)	y_A	$k_o\tau$	$k_o \times 10^8$ (m/min)	k_d (m^3/kmol · min)	r^2 (−)
30	15	2	0.15	7.278 (±0.003)	6.151	0.074 (±0.001)	0.997
30	35	2	0.15	3.019 (±0.004)	5.960	0.093 (±0.002)	0.997
30	35	2	0.15	4.523* (±0.005)	8.930*	0.064* (±0.004)	0.996
30	60	2	0.15	1.738 (±0.002)	5.882	0.086 (±0.003)	0.996
30	35	1	0.15	1.534 (±0.003)	6.057	0.082 (±0.002)	0.998
30	35	2	0.15	3.019 (±0.004)	5.960	0.093 (±0.002)	0.997
30	35	3	0.15	4.395 (±0.002)	5.785	0.101 (±0.004)	0.998
30	35	2	0.05	2.911 (±0.004)	5.747	0.087 (±0.002)	0.996
30	35	2	0.15	3.019 (±0.004)	5.960	0.093 (±0.002)	0.997
30	35	2	0.50	3.114 (±0.002)	6.148	0.106 (±0.004)	0.998
30	35	2	0.15	3.019 (±0.004)	5.960	0.093 (±0.002)	0.997
40	35	2	0.15	3.787 (±0.002)	7.477	0.288 (±0.001)	0.999
50	35	2	0.15	4.489 (±0.003)	8.863	1.004 (±0.003)	0.998

The asterisk symbol (*) means adsorption with moisture.

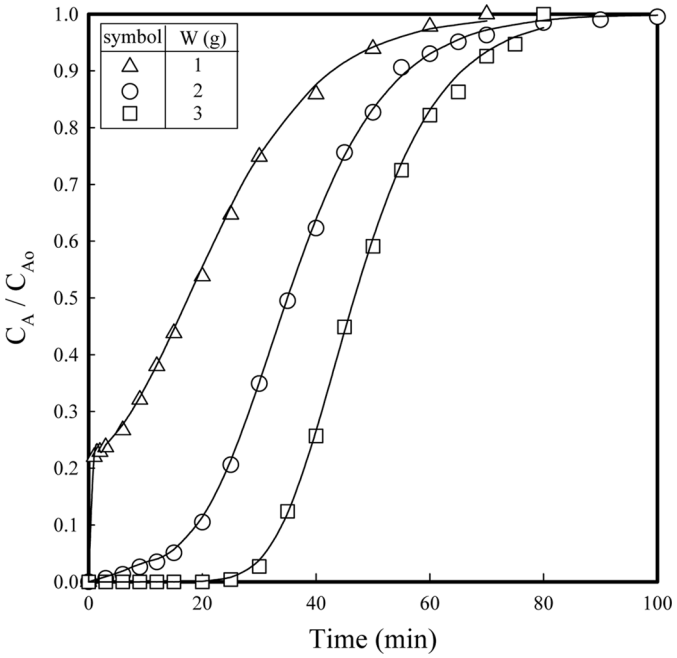

FIG. 4. Effect of amount of adsorbent on the breakthrough curve of CO_2. ($Q_o = 35\,cm^3/min$, $y_A = 0.15$, $T = 30°C$).

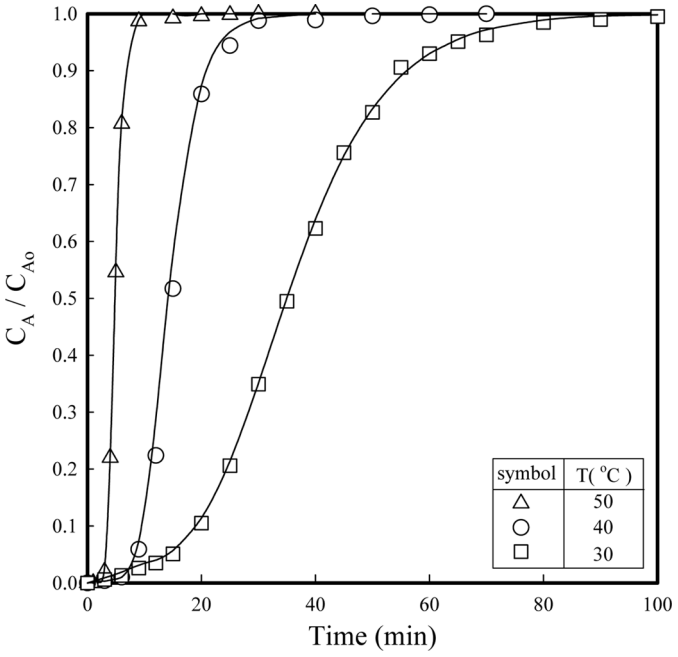

FIG. 6. Effect of CO_2 concentration on the breakthrough curve of CO_2. ($Q_o = 35\,cm^3/min$, $W = 2\,g$, $T = 30°C$).

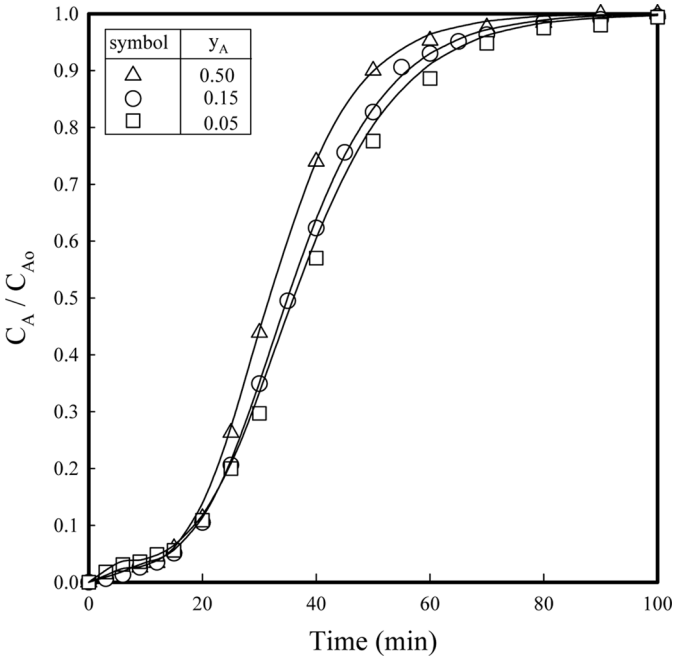

FIG. 5. Effect of adsorption temperature on the breakthrough curve of CO_2. ($Q_o = 35\,cm^3/min$, $W = 2\,g$, $y_A = 0.15$).

Effect of Adsorption Temperature

To investigate the effect of adsorption temperature on the adsorption kinetics, the breakthrough curves of CO_2 were measured in the range of temperature from 30–50°C. The measured outlet concentrations of CO_2 were typically plotted against the adsorption time for the various temperatures indicated as various symbols in Fig. 6 under the typical experimental conditions of $35\,m^3/min$ of the gaseous mixture and 2 g of EDA-CP-MS41. The model parameters were evaluated by analysis of the experimental breakthrough data using a nonlinear least squares technique and were tabulated in Table 1. The results in Fig. 6 indicated a shift in breakthrough curves toward the left with increased temperature, which might be attributed to an increase in the amount of adsorbed CO_2 due to increase of reaction and deactivation and was the same result of the breakthrough curves of trichloroethylene vapor on activated carbon (31). Arrhenius plots of k_o and k_d were shown in Fig. 7. The activation energy for the adsorption (ΔE_a) and deactivation (ΔE_d) were obtained from the slopes of plots in Fig. 7, and their values were 16.2 and 96.7 kJ/mole, mole, respectively.

Adsorption Accompanied with Chemical Reaction

Although it has been shown that there are a variety of species formed in adsorption of CO_2 onto amine-modified silica gel, as reported in Chang et al. (22), some authors (18, 20) present the simple mechanism. In this study, the adsorption of CO_2 onto the solid particles with and without moisture was assumed simply to occur as shown in Fig. 8 (18).

The surface interaction of CO_2 with EDA-CP-MS41 was confirmed using FT-IR spectrums as follows: IR bands were

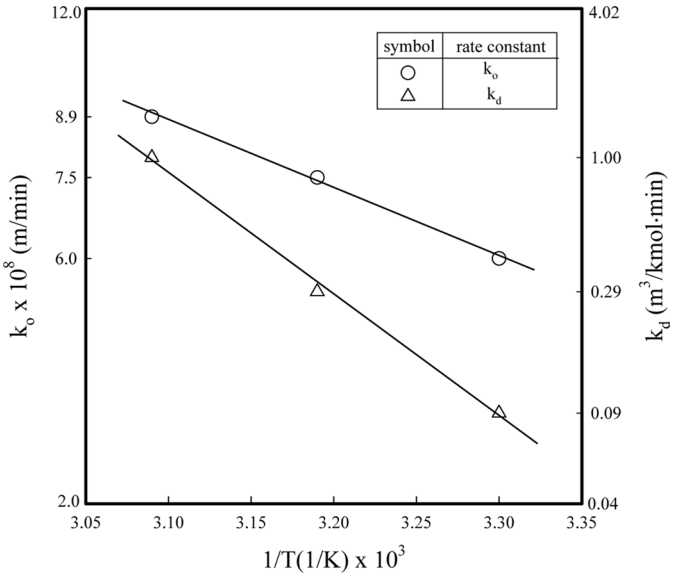

FIG. 7. Effect of adsorption temperature on dimensionless absorption rate constant and deactivation rate constant.

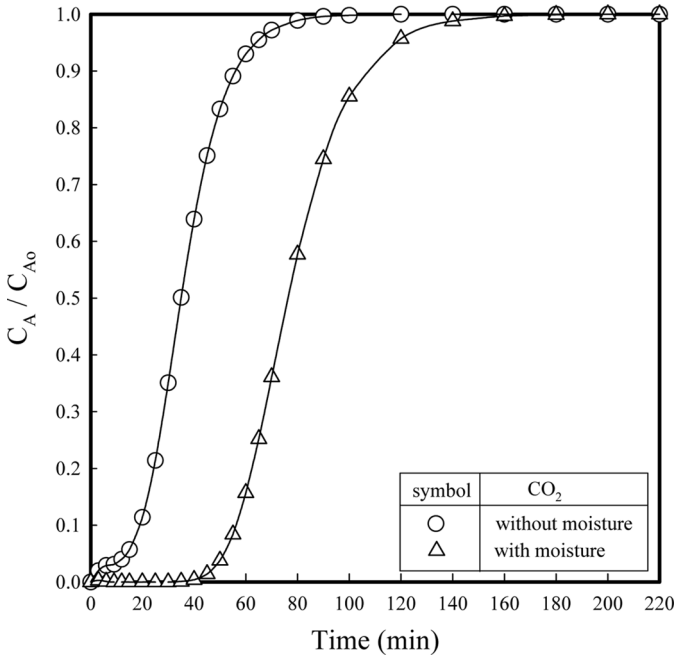

FIG. 9. Effect of moisture on the breakthrough curve of CO_2. ($Q_o = 35\,cm^3/min$, $y_A = 0.15$, $W = 2\,g$, $T = 30°C$).

complicatedly observed in the range of 1700–1300 cm^{-1}; adsorbed gaseous CO_2 (1330 cm^{-1}), bicarbonate in C-O bending (1382 cm^{-1}), carbamate in C-O bending (1432 and 1485 cm^{-1}), and NH_3^+ (1560 and 1635 cm^{-1}). From these results, the surface interaction of CO_2 with the amine-modified samples (EDA-CP-MS41) was confirmed. These results were the same as those of Huang et al. (20).

The breakthrough curves of CO_2 were measured at CO_2 concentration of 15%, the flow rate of the gaseous mixture of 35 cm^3/min, temperature of 30°C, and EDA-CP-MS41 of 2 g with and without water moisture in Fig. 9.

As shown in Fig. 9, the breakthrough curve shifts toward the right with water moisture, and $k_o\tau$ and k_d, tabulated in Table 1, were 4.523 and 0.064 m^3/kmol · min, respectively. This $k_o\tau$ was larger than that without water moisture and the k_d, smaller than that without moisture.

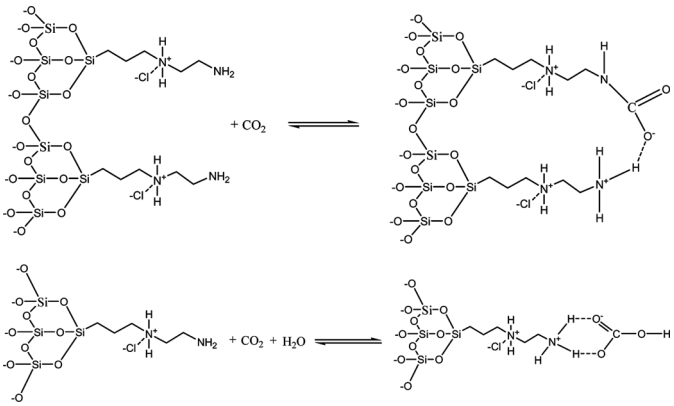

FIG. 8. Surface reaction mechanism of CO_2 without and with moisture for adsorption of CO_2 onto EDA-CP-MS41.

The upper area of the breakthrough curve of CO_2 was integrated according to the adsorption stream time to evaluate the weight change of CO_2, which was shown in Fig. 9. The amount of CO_2 adsorbed with moisture was 555 mg/g-adsorbent, which was 86% larger than 298 mg/g-adsorbent during 200 minutes. The adsorption should increase about two times in the presence of water, but, it was about 1.86 times. This value may be acceptable figures from the engineering point of view with experimental error.

Comparison of the Proposed Models

Several equilibrium models (28), which have been developed to describe adsorption isotherm relationships, are useful for describing adsorption capacity and theoretical evaluation of thermodynamic parameters, such as heats of adsorption. But, sometimes the experimental procedure to prepare the adsorption isotherm relationships is very tedious and takes too much time. The equilibrium concentrations between two phases, which are used to describe the adsorption isotherm relationships, can be obtained by Eq. (5) and (6), where a(t), x and y are the dimensionless concentrations of CO_2 in the breakthrough data (36), in the gas phase and solid phase, respectively.

$$x = \frac{\int_o^t a(t)dt}{\int_o^\infty a(t)dt} \tag{5}$$

$$y = \frac{t - x\int_o^\infty a(t)dt}{\int_o^\infty dt - x\int_o^\infty a(t)dt} \tag{6}$$

TABLE 2
Selected adsorption isotherms to fit the breakthrough data of CO_2 for comparison with the deactivation model

Adsorption isotherms	Mathematical representation of adsorption isotherms	Linearized forms	Parameters and correlation coefficient
Langmuir	$y = \frac{ax}{(1+bx)}$	$\frac{1}{y} = \frac{1}{ax} + \frac{b}{a}$	$a = 15.678$ $b = 12.897$ $r^2 = 0.897$
Freundlich	$y = ax^b$	$\ln(y) = \ln(a) + b\ln(x)$	$a = 1.2323$ $b = 0.4092$ $r^2 = 0.925$
Brunauer-Emmett-Teller	$y = \frac{x}{(1-x)(a+bx)}$	$\frac{x}{y(1-x)} = a + bx$	$a = -0.4415$ $b = 5.7137$ $r^2 = 0.453$
Dubinin-Radshkevich-Kagener	$y = a\ \exp[-b\ln^2(x)]$	$\ln(y) = \ln(a) - b\ln^2(x)$	$a = 0.9487$ $b = 0.0844$ $r^2 = 0.987$
Deactivation model (this study)	x according to Eq. (5) y according to Eq. (6)		$k_S\tau = 3.019$ $k_d = 0.093$ $r^2 = 0.994$

As shown in Eq. (5) and (6), the ranges of x and y are between 0 and 1, respectively. The equilibriums for single-solute sorption given in the literature (28) are frequently presented as dimensionless concentration isotherms. To compare the deactivation model with the equilibrium isotherm models, models selected by Suyadal et al. (31) were used as follows; Langmuir, Freundlich, BET, and DRK model, whose formulas were listed in Table 2. The typical experimental conditions indicated as circle were used, i.e., a gaseous flow rate of $35\,cm^3/min$,

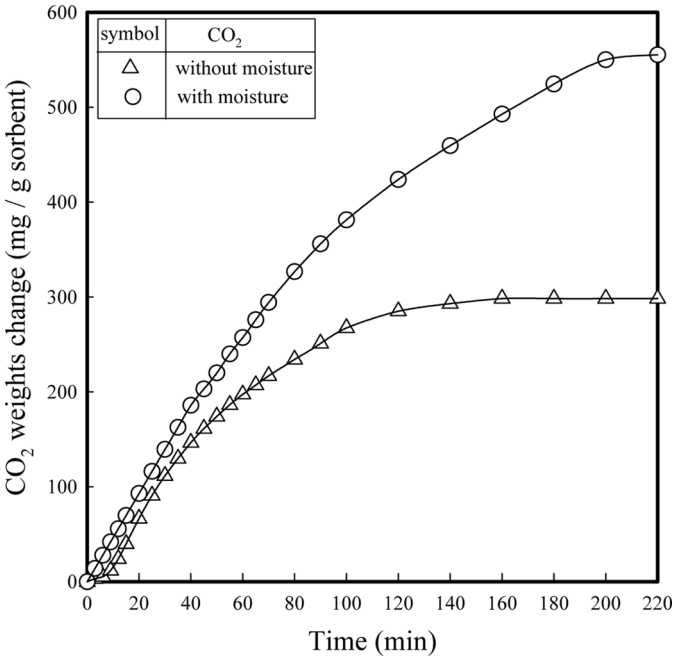

FIG. 10. Amount of CO_2 adsorbed with/without moisture under the same experimental conditions in Fig. 9.

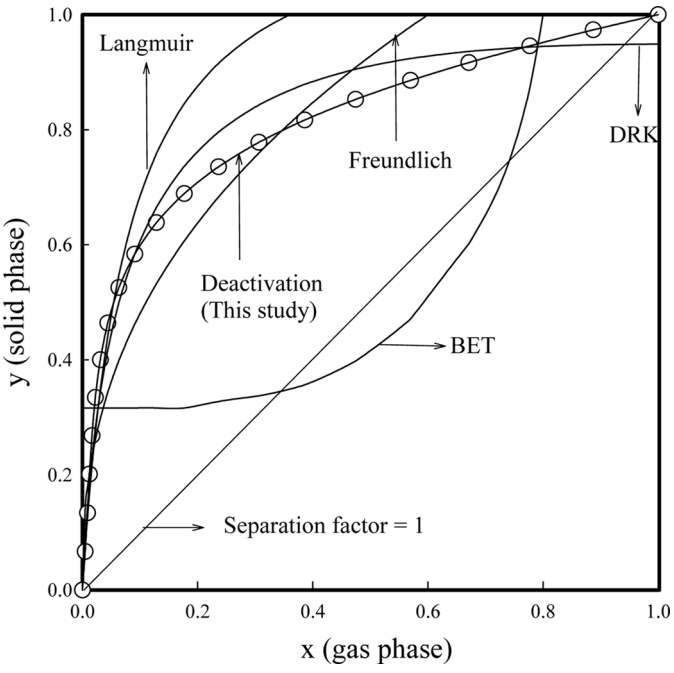

FIG. 11. Comparison of the model in describing the experimental breakthrough curve of CO_2 according to Table 2 under the same experimental conditions in Fig. 9.

amounts of EDA-CP-MS41, 2 g, and adsorption temperature, 30°C. Using a(t) obtained from the experimental parameters, the values of x and y obtained from Eq. (5) and (6), were shown in Fig. 11 and used to obtain to give the constants of a and b in each model.

As shown in Table 2 and Fig. 11, the proposed deactivation model fitted the data with the highest correlation (r^2) of 0.994, and the adsorption of CO_2 on EDA-CP-MS41 might be favorable isotherms due to the separation factor less than unity. Failure of BET, Langmuir, DRK, and Freundlich model in order in the fitting with the experimental data in Fig. 10 may be explained by the gas-solid heterogeneous reaction containing adsorption between CO_2 and EDA-CP-MS41.

CONCLUSIONS

Mesoporous EDA-CP-MS41 was used as an adsorbent to capture CO_2 and the breakthrough data were measured in a fixed bed to observe the adsorption kinetics. The adsorption kinetics was assumed to be the first-order with respect to the concentration of CO_2 and the activity of the adsorbent, respectively. The adsorption and deactivation rate constant were evaluated by the deactivation model through analysis of the experimental breakthrough data using a nonlinear least squares technique. Moisture actually increased the CO_2 adsorption capacity because of the special chemical reaction mechanism between CO_2 and amines in EDA-CP-MS41. The experimental breakthrough data were fitted very well to the deactivation model than the adsorption isotherm models in the literature.

NOMENCLATURE

a	ratio of outlet concentration of CO_2 to inlet concentration
C_A	outlet concentration of CO_2 in gaseous stream
C_{Ao}	inlet concentration of CO_2 in gaseous stream
k_d	deactivation rate constant ($m^3/kmol \cdot min$)
k_o	adsorption rate constant (m/min)
m	deactivation order in Eq. (2)
n	adsorption order in Eq. (2)
Q_o	flow rate of gaseous mixtures of N_2 and CO_2(m^3/min)
r^2	correlation coefficient
S	surface area of adsorbent (m^2)
t	adsorption time (min)
T	adsorption temperature (K)
x	dimensionless concentrations of CO_2 in gas phase through the sorption isotherm
y	dimensionless concentrations of CO_2 in solid phase through the sorption isotherm
y_A	mole fraction of CO_2
W	amount of adsorbent (g)

Greek Letters

α	activity of the solid adsorbent
τ	surface-time defined as ratio of S to Q_o(min/m)

Subscript

A	CO_2

ACKNOWLEDGMENTS

This work was supported by Brain Korea 21 Project and a grant (2006-C-CD-11-P-03-0-000-2007) from the Energy Technology R&D of Korea Energy Management Corporation. Dae-Won Park is also thankful for KOSEF (R01-2007-000-10183-0).

REFERENCES

1. Aresta, M. (2003) *Carbon Dioxide Recovery and Utilization*; Kluwer Academic Pub.: Boston.
2. Bartoo, R.K. (1984) Removing acid gas by the benfield process. *Chem. Eng. Prog.*, *80*: 35.
3. Ruhl, M.L. (1993) Recover of VOCs via adsorption on activated carbon. *Chem. Eng. Prog.*, *89*: 1344.
4. Kresge, C.T.; Leonowicz, M.E.; Roth, W.J.; Vartuli, J.C.; Beck, J.S. (1992) Ordered mesoporous molecular sieves synthesized by a liquid-crystal template mechanism. *Nature*, *359*: 710.
5. Beck, J.S.; Vartuli, J.C.; Roth, W.J.; Leonowicz, M.E.; Kresge, C.T.; Schmitt, K.D.; Chu, C.T.W.; Olson, D.H.; Sheppard, E.W.; McCullen, S.B.; Higgins, J.B.; Schlenker, J.L. (1992) A new family of mesoporous molecular sieves prepared with liquid crystal templates. *J. Am. Chem. Soc.*, *114*: 10834.
6. Bhaumik, A.; Tatsumi, T. (2000) Organically modified titanium-rich Ti-MCM-41, efficient catalysts for epoxidation reactions. *J. Catal.*, *189*: 31.
7. Burkett, S.L.; Sim, S.D.; Mann, S.J. (1996) Synthesis of hybrid inorganic-organic mesoporous silica by co-condensation of siloxane and organicsiloxane precursors. *J. Chem. Soc. Chem. Commun.*, 1367.
8. Lim, M.H.; Blanford, C.F.; Stein, A. (1997) Synthesis and characterization of a reactive vinyl-functionalized MCM-41: Probing the internal pore structure by a bromination reactions. *J. Am. Chem. Soc.*, *119*: 4090.
9. Zhao, D.; Feng, J.; Huo, Q.; Melosh, N.; Fredrickson, G.H.; Chmelka, B.F.; Stucky, G.D. (1998) Triblock copolymer syntheses with periodic 50 to 300 angstrom pores. *Science*, *279*: 548.
10. Fowler, C.E.; Lebeau, B.; Mann, S. (1998) Covalent coupling of an organic chromophore into functionalized MCM-41 mesophases by template-directed co-condensation. *J. Chem. Soc. Chem. Commun.*, 1825.
11. Babonneau, F.; Leite, L.; Fontlupt, S. (1999) Structural characterization of organically-modified porous silicates synthesized using CTA^+ surfactant and acidic conditions. *J. Mater, Chem.*, *9*: 175.
12. Abramson, S.; Lasperas, M.; Galaneau, A.; Desplantie-Giscard, D.; Brunel, D. (2000) Best design of heterogenized β-aminoalcohols for improvement of enantioselective addition of diethylzinc to benzaldehyde. *Chem. Communication*, 1773.
13. Sakthivel, A.; Sun, W.; Raudasschl-Sieber, G.; Chiang, A.S.T.; Hanzik, M.; Kuhn, F.E. (2006) Grafting of a tetrahydro-salen copper(II) complex on surface modified mesoporous materials and its catalytic behaviour. *Catal. Communication*, *7*: 302.
14. Lou, L.L.; Yu, K.; Ding, F.; Peng, X.; Dong, M.; Zhang, C.; Liu, S. (2007) Covalently anchored chiral Mn(III) salen-containing ionic species on mesoporous materials as effective catalysts for asymmetric epoxidation of unfunctionalized olefins. *J. Catal.*, *249*: 102.

15. Soundiressane, T.; Selvakumar, S.; Menage, S.; Hamelin, O.; Fountecave, M.; Singh, A.P. (2007) *N,N′*-bis(2-pyridylmethyl)-*N*-methyl-(1S,2S)-1,2-cyclohexanediamine complexes immobilized on mesoporous MCM-41: Synthesis, characterization and catalytic applications. *J. Mol. Catal.*, *270*: 132.
16. Udayakumar, S.; Son, Y.S.; Lee, M.Y.; Park, S.W.; Park, D.W. (2008) The synthesis of chloropropylated MCM-41 through co-condensation technique: The path finding process. *Applied Catalysis A: General*, *347*: 192.
17. Burwell, R.L.; Leal, O. (1974) Modified silica gel as selective adsorbents for sulfur dioxide. *Chem. Communication*, 342.
18. Leal, O.; Bolivar, C.; Ovalles, C.; Garcia, J.J.; Espidel, Y. (1995) Reversible adsorption of carbon dioxide on amine surface-bounded silica gel. *Inorganica Chimica Acta*, *240*: 183.
19. Satyapal, S.; Filburn, T.; Trela, J.; Strange, J. (2001) Performance and properties of a solid amine sorbent for carbon dioxide removal in space life support application. *Energy & Fuels*, *15*: 250.
20. Huang, H.Y. Yang, R.T. (2003) Amine-grafted MCM-48 and silica xerogel as superior sorbents for acidic gas removal from natural gas. *Ind. Eng. Chem. Res.*, *42*: 2427.
21. Xu, X.; Song, C.; Andreson, J.M.; Miller, B.G.; Scaroni, A.W. (2002) Novel polyethylenimine-modified mesoporous molecular sieve of MCM-41 as high-capacity. Adsorbent for CO2 capture. *Energy & Fuels*, *16*: 1463.
22. Chang, A.C.C.; Chuang, S.S.C.;, Gray, M.; Soong, Y. (2003) In-situ infrared study of CO2 adsorption on SBA-15 grafted with γ-(aminopropyl)triethoxysilane. *Energy & Fuels*, *17*: 468.
23. Zhao, H.; Hu, J.; Wang, J.; Xhou, L.; Liu, H. (2007) CO_2 capture by the amine-modified mesoporous materials. *Acta Physico-Chimica Sinica*, *23*: 801.
24. Udayakumar, S.; Park, S.W.; Park, D.W.; Choi, B.S. (2008) Immobilization of ionic liquid on hybrid MCM-41 system for the chemical fixation of carbon dioxide on cyclic carbonate. *Catal. Commun.*, *9*: 1563.
25. Doraiswamy, L.K.; Sharma, M.M. (1954) *Heterogeneous Reactions*; John Wiley & Sons: New York.
26. Orbey, N.; Dogu, G.; Dogu, T. (1982) Breakthrough analysis of non-catalytic solid-gas reaction: Reaction of SO_2 with calcined limestone. *Can. J. Chem. Eng.*, *60*: 314.
27. Ruthven, D.M. (1984) *Principles of Adsorption and Adsorption Processes*; John & Wiley: New York.
28. Suzuki, M. (1990) *Adsorption Engineering*; Kodansga Ltd: Tokyo.
29. Yasyerli, S.; Dogu, T.; Dogu, G.; Ar, I. (1996) Deactivation model for textural effects on kinetics of gas-solid noncatalytic reactions "char gasification with CO_2. *Chem. Eng. Sci.*, *51*: 2523.
30. Kopac, T.; Kocabas, S. (2003) Sulfur dioxide adsorption isotherms and breakthrough analysis on molecular sieve 5A. *Chem. Eng. Comm.*, *190*: 1041.
31. Suyadal, Y.; Erol, M.; Oguz, M. (2000) Deactivation model for the absorption of trichloroethylene vapor on an activated carbon. *Ind. Eng. Chem. Res.*, *39*: 724.
32. Park, S.W.; Sung, D.W.; Choi, B.S.; Oh, K.W. (2006) Sorption of carbon dioxide onto sodium carbonate. *Sep. Sci. Technol.*, *41*: 2665.
33. Park, S.W.; Sung, D.W. Choi, B.S.; Lee, J.W.; Kumazawa, H. (2006) Carbonation kinetics of potassium carbonate by carbon dioxide. *J. Ind. Eng. Chem.*, *12*: 522.
34. Park, S.W.; Choi, B.S.; Lee, J.W. (2007) Breakthrough data analysis of adsorption of toluene vapor in a fixed-bed of granular activated carbon. *Sep. Sci. Technol.*, *42*: 2221.
35. Dogu, T. (1986) Extension of moment analysis to nonlinear systems. *AIChE J.*, *32*: 849.
36. Yasyerli, S.; Dogu, G.; Ar, I. (2003) Breakthrough analysis if H_2S removal on Cu-V-Mo, Cu-V, and Cu-Mo mixed oxides. *Chem. Eng. Comm.*, *190*: 1055.